Journal of Fluorescence (2022) 32:2271–2280
https://doi.org/10.1007/s10895-022-03017-x

RESEARCH

Synthesis of Orange-Red Emissive Au-SG and AuAg-SG Nanoclusters and Their Turn-OFF vs. Turn-ON Metal Ion Sensing

Sagar Bhowmik[1,2] · Shashikana Paria[1] · Ishika Tater[1] · Prasenjit Maity[1,2]

Received: 8 June 2022 / Accepted: 19 August 2022 / Published online: 7 September 2022

Abstract

Synthesis of luminescent metal cluster for selective sensing of specific analyte with detail mechanistic understanding is very important for real world applications as well as for developing new emissive materials. In the present work, we have synthesized L-glutathione stabilized gold (Au-SG) and gold-silver bimetallic (AuAg-SG) clusters under identical experimental conditions with orange red emissive characteristics for both. Detail photo physical analysis reveals that both clusters are phosphorescent in nature with moderate quantum yield of 7% and 19% for Au-SG and AuAg-SG respectively and their excited state lifetime values are in the range of 1–2 µs. While Au-SG cluster showed luminescence quenching response (turn-off) in presence of Fe^{3+} and Hg^{2+} ions, AuAg-SG cluster showed turn-off response for Cu^{2+}, Fe^{3+} and Hg^{2+}, but luminescent enhancement (turn-on) response for Cd^{2+} ions. The highest detection limit obtained for Cu^{2+} ion by AuAg-SG cluster is 20 nM while for Cd^{2+} ion it is 75 nM. From Time Correlated Single Photo Counting (TCSPC) and Dynamic Light Scattering (DLS) measurements we postulated that except Cd^{2+}, all other metal ions cause aggregation of clusters through ligation with SG ligands while Cd^{2+} ion does not induce any cluster aggregation but binds to cluster surface atoms. The near constant life time values of both clusters during gradual addition of respective metal ions confirms static quenching/enhancement process through formation of stable ground state adducts.

Keywords Metal ion sensing · Luminescence · Metal cluster · Turn ON · Turn OFF · TCSPC

Introduction

Ligand stabilized ultra-small coinage metal clusters have emerged as a new class of functional material with unique physico-chemical properties and have tremendous application potential specially in the areas of trace level sensing, bio-imaging, light emitting diodes and catalysis [1–5]. These small clusters show molecular like optical absorption properties, high quantum yield and tuneable luminescence behaviour with good photo stability, selective catalytic activity and good bio-compatibility which make them superior than the organic dye/fluorophores [6–8]. The origin of emission from these clusters are broadly decided by the nature of metal(s) and their oxidation state, size of the cluster, atomic arrangement of the cluster, type of ligand and metal–ligand interfacial structure [7–10]. Strong luminescence, large stokes shift, high photo-thermal stability, good biocompatibility, availability of easy surface modification routes and their high stability under ambient conditions are reasons behind their potential applications [7–11]. These qualities has driven strong interest to pursue development metal nanocluster (NC) based selective and sensitive luminescence sensor for various analytes under aqueous phase in ambient conditions. The use of stabilizing ligands with various surface functional groups, e.g., thiol, alkyne, halide, carbene, amine and carboxylic acids have been studied to synthesize a variety of emissive clusters [12–18]. Although various ligands have been successfully used, but still the "thiol" based ligands including small thiol molecules, amino acids, peptides and proteins are found most intriguing in terms of synthesizing highly emissive metal clusters. L-Glutathione is a tripeptide with a free-SH group and have been used extensively to synthesize a variety of metal clusters and nanoparticles [19–26]. The highly fluorescent $Au_{22}(SG)_{18}$ cluster with strong red emission is one of the most prominent early example with a quantum yield of

✉ Prasenjit Maity
prasenjit.maity@nfsu.ac.in

[1] School of Engineering and Technology, National Forensic Sciences University - Gandhinagar, Sector-09, Gandhinagar 382007, India

[2] School of Forensic Science, National Forensic Sciences University - Tripura, Radhanagar, Agartala 799001, India

16% [20, 21]. It was revealed that aggregation of Au(I)-SG oligomers on Au(0) kernel induced ligand to metal charge transfer (LMCT) transitions for showing such strong emission [20, 21]. In pursuit of isolating more emissive cluster, alloying of two metals were tested as the resulting bimetallic cluster may achieve higher quantum yield through better geometrical rigidity, smaller kernel size and efficient electron transfer dynamics [27–39]. Thus, alloying of Ag or Cu with Au have resulted a number of highly luminescent bimetallic clusters in recent years with high quantum yield up to 71% [33].

Trace level detection of various analytes including metal ions, explosives, specific biomolecules, toxic molecules and food contaminants by luminescent noble metal clusters is a promising approach [40–45]. The detection of trace quantity of metal ions is important as their contamination in food, drinking water and in body fluids is very important from human health safety and diagnostic prospective. The advantages of luminescence sensing of analytes includes very high sensitivity and selectivity, low cost, on the spot testing feasibility and fast response time [40] Luminescence quenching (Turn-OFF) is the most dominant pathway of sensing analytes demonstrated by various metal clusters and we may ascribe its origin through electron/energy transfer from metal cluster to analyte through a static or dynamic adduct formation mechanism [46–50]. Luminescence enhancement (Turn-ON) based sensing of analytes is more advantageous but is less common and it follows a distinct mechanism than the previous one [51–53]. Thus, one of the major motivation of the work is to develop metal NC based turn-on sensors for specific metal ions and understanding the underlying mechanism behind it. In metal ion sensing, the ions may interact with surface ligands, or it may interact with surface metal atoms of the cluster and may also form a different alloy resulting a luminescence response. Hence, we were interested to understand the metal ion sensing ability of a monometallic (Au_n) and a bimetallic nanocluster (Au_nAg_m) stabilized by a sufficiently polar thiol ligand {L-Glutathione (L-GSH)}. We anticipated that various metal ions will interact differently with mono and bimetallic nanocluster surface atoms or with the ligand functional groups and may result different responses. Thus, the present work reports synthesis, characterization and luminescence sensing behaviour of Glutathione stabilized Au and AuAg clusters for various metal ions with a major focus on their photo physical aspects. Interestingly, we could find that while gold clusters showed selective luminescence quenching based sensing of Fe^{3+} and Hg^{2+}, the AuAg cluster showed luminescence quenching for Fe^{3+}, Hg^{2+} and Cu^{2+} but luminescence enhancement in presence of Cd^{2+}. Detailed steady state emission behaviour and TCSPC analysis were performed along with hydrodynamic diameter (D_h) to understand this different sensing behaviour for two different clusters. The present work is also significant for the observed turn-on luminescence response of the bimetallic cluster and may find application as a real world sensor for the detection of trace level metal ions. In addition to it the work suggests that it may be feasible to synthesize a tri-metallic cluster with high phosphorescence quantum yield at room temperature by combining Au, Ag and Cd.

Experimental Section

Materials and Instruments

Gold (III) chloride trihydrate ($HAuCl_4.3H_2O$), Silver nitrate ($AgNO_3$), L-Glutathione, Sodium hydroxide (NaOH), Ferric nitrate ($Fe(NO_3)_3$, Cadmium chloride ($CdCl_2$), Copper nitrate ($Cu(NO_3)_2$, $3H_2O$), Zinc chloride ($ZnCl_2$), Mercury (II) nitrate ($Hg(NO_3)_2$), Chromium (III) chloride ($CrCl_3$, $3H_2O$), Lead chloride ($PbCl_2$), Arsenic (III) oxide (As_2O_3), Cobalt (II) nitrate ($Co(NO_3)_2$), Manganese (II) chloride ($MnCl_2$), Nickel (II) chloride ($NiCl_2$), Ammonium chloride (NH_4Cl), Potassium bromide (KBr), Sodium chloride (NaCl) were obtained from Sigma-Aldrich Chemical Co. Milli-Q grade water were used in all experiments. UV–Vis spectroscopic measurements were performed in a JASCO V-670 spectrophotometer. All the solution phase photoluminescence spectra were obtained by using a HORIBA Fluoromax spectrofluorometer at 298 K. Dynamic light scattering (DLS) experiments for measuring hydrodynamic diameter were performed by using a Malvern DLS instrument (Zetasizer Nano ZSP model). HORIBA Jobin Yvon Deltaflex time correlated single photon counting (TCSPC) spectrophotometer was used for recording phosphorescence (PL) decays. The samples were excited at 370 nm by a spectral LED (model Spectra LED-370). Transmission electron microscopic (TEM) images were recorded by using a Philips JEM 2000FX electron microscope operated at 200 kV. Matrix Assisted Laser Desorption Ionisation (MALDI) mass spectra were recorded by using a time-of-flight (TOF) mass spectrometer (Bruker, Autoflex Speed) operated with a solid state laser (355 nm, 3 Hz, < 100 mJ). Inductively Coupled Plasma-Optical Emission Spectrometry (ICP-OES) analysis was performed in a Thermo Fischer instrument (iCAP Pro ICP-OES). Energy Dispersive X-Ray Fluorescence (ED-XRF) analysis was performed on a Shimadzu instrument (Model EDX-7000/8100).

Synthesis of Au-SG and AuAg-SG Cluster

The synthesis of Au-SG and AuAg-SG cluster were performed by following a literature reported procedure with minor modifications [54]. First we prepared a stock solution of 100 mM L-Glutathione (L-GSH), 15 mM of $HAuCl_4$ and 15 mM of $AgNO_3$ in three separate vials. For the synthesis of AuAg Cluster, we mixed 0.45 mL of L-GSH solution, 1.35 mL of $HAuCl_4$ solution and 0.15 mL of $AgNO_3$ solution

in a clean and dry round bottom flask with another additional 30 mL of Milli-Q water. Then NaOH (1 M, 60µL) was added drop wise in that mixture to fix the final pH of the solution at 7. Afterwards, this round bottom flask (RB) was placed in an oil bath at 85 °C under stirring (600 rpm) and fitted with a reflux condenser for 6 h. The solution was then cooled to room temperature, purified using membrane filter (3000 Da) under high speed centrifugation (10,000 rpm) to get concentrated solution and finally dried using a fridge dryer. The Au-SG cluster was prepared under identical conditions without addition of $AgNO_3$ in the reaction mixture.

Metal Ion Sensing Procedure

First the respective metal salts were dissolved in Milli-Q water with a final concentration of 2.65 mM. For preparation of aqueous metal cluster solutions, 1 mg of dried cluster was dissolved in 10 mL of Milli-Q water (100 ppm) and it was used as stock solution. Then 2 mL of the stock solution of the respective clusters were taken in a cuvette and the steady state luminescence spectra were recorded during gradual addition (10 µL at a time) of these metal salt solutions. Excitation wavelength was fixed at 395 nm for Au-SG cluster and 396 nm for AuAg-SG cluster.

Results and Discussion

Synthesis, Characterization and Optical Properties of Au-SG and AuAg-SG Clusters

Synthesis of monometallic Au-SG cluster and AuAg-SG bimetallic cluster were accomplished through a hustle free hydrothermal procedure under neutral pH and a 9:1 molar ratio of Au:Ag was maintained for the bimetallic cluster. The purified clusters were characterized by UV–Vis, PL, TCSPC, TEM, DLS and MALDI techniques. The representative TEM images and MALDI mass spectra for these two clusters are presented in Fig. 1. Highly mono-disperse ultra-small particles with average diameter of 1.2 ± 0.2 nm were observed for both the clusters (Fig. 1a, b). Mass spectrometric analysis of both clusters were also measured, which showed the major molecular peak (weight) of 5.1 kDa and 4.8 kDa for Au-SG and AuAg-SG clusters respectively (Fig. 1c, d). However, the broad mass spectral pattern with abundance of few other smaller peaks indicate that in molecular level these clusters are poly dispersed. The average hydrodynamic diameter (D_h) for these two clusters dispersed in water media were also measured by dynamic light scattering (DLS) technique to get an idea about their solution phase behaviour and stabilities. We observed that their hydrodynamic diameter is very identical (~2.5 nm), which indicates their good aqueous dispersion and non-aggregation nature. The higher hydrodynamic diameter

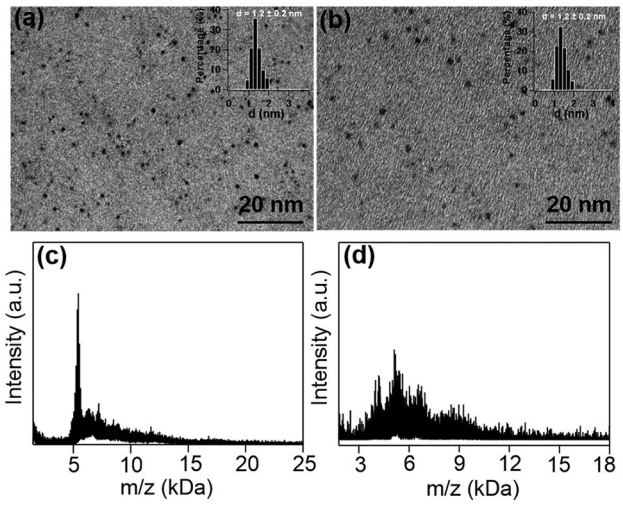

Fig. 1 TEM images with particle size histograms (**a**, **b**) and MALDI mass spectra (**c**) and (**d**) of Au-SG cluster and AuAg-SG cluster respectively

as compared to diameter observed from TEM measurement is quite expected as the associated ligand and solvents surrounding the metal cluster makes D_h value larger.

Next the solution phase optical (UV–Vis) absorption spectra and emission spectra were recorded for these two clusters at room temperature (298 K). Both clusters exhibit strong UV light absorption profiles as the absorbance increases strongly in the UV region as compared to visible region of the spectra (Fig. 2). Both clusters showed strong orange-red emission under 365 nm UV light source (Fig. 2, inset). Hence, we systematically analysed their solution phase emission behaviour and first measured 3D emission profiles to know exact excitation and emission wavelengths (Figs. S1 and S2). The optimized λ_{ex} and λ_{emi} values for Au-SG cluster are 395 nm and 585 nm respectively and for AuAg-SG cluster, the excitation and emission wavelengths are 396 nm and 605 nm respectively (Fig. 2). Thus, a relatively large stokes shift of 190 nm and 207 nm were observed for Au-SG and AuAg-SG clusters. The quantum yield measured through integrated sphere methods were 7% and 19% respectively, which could be considered high for metal clusters. The luminescence decay profiles for both the clusters were measured to calculate the excited state lifetime values (Figs. 3, S3 and Table 1). The best fitted decay profiles for both the clusters gave two lifetime components, 0.26 µs (86%) and 2.84 µs (14%) with an average τ value of 0.62 µs for Au-SG cluster. For AuAg-SG cluster, the life time values are 0.71 µs (62%) and 2.77 µs (38%) with an average τ value of 1.49 µs. Such long luminescence lifetime values in the microsecond range indicates that the emission of both these clusters are phosphorescence in nature. We may

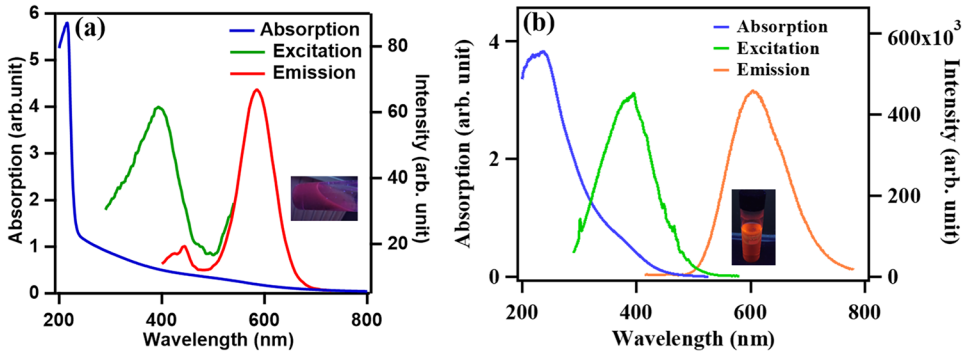

Fig. 2 Room temperature solution phase (aqueous) UV–Vis spectra, excitation spectra and emission spectra of Au-SG cluster (**a**) and AuAg-SG cluster (**b**); the inset figure shows the solution phase colour of the respective clusters upon illumination under 365 nm UV lamp

attribute the origin of such emission to ligand-to-metal charge transfer (LMCT) or ligand-to-metal–metal charge transfer (LMMCT) based excitation followed by emission via metal-centered triplet excited state [22]. The stability of the AuAg-SG cluster with respect to pH, UV light and oxygen purging and its excitation wavelength dependent emission spectra were also measured (Figs. S4, S5, S6, S7 and S8). The emission wavelength remains same upon excitation with varying wavelength (340 to 450 nm range), indicating the fixed band gap of 605 nm but the intensity is found to be highest with excitation wavelength of 396 nm. The emission intensity decreases while purging oxygen gas through the cluster solution, which again confirms the involvement of triplet state as emissive state. The emission is quite stable under dark conditions as well as under UV light irradiation, indicating its stability against photo bleaching. The emission of AuAg cluster is enhanced at low pH possibly due to influence of ligands through attending specific packing surrounding the cluster.

Metal Ion Sensing by Au-SG and AuAg-SG Clusters

The major emphasis of the present work was to find out the differential sensing behaviour of these two clusters for

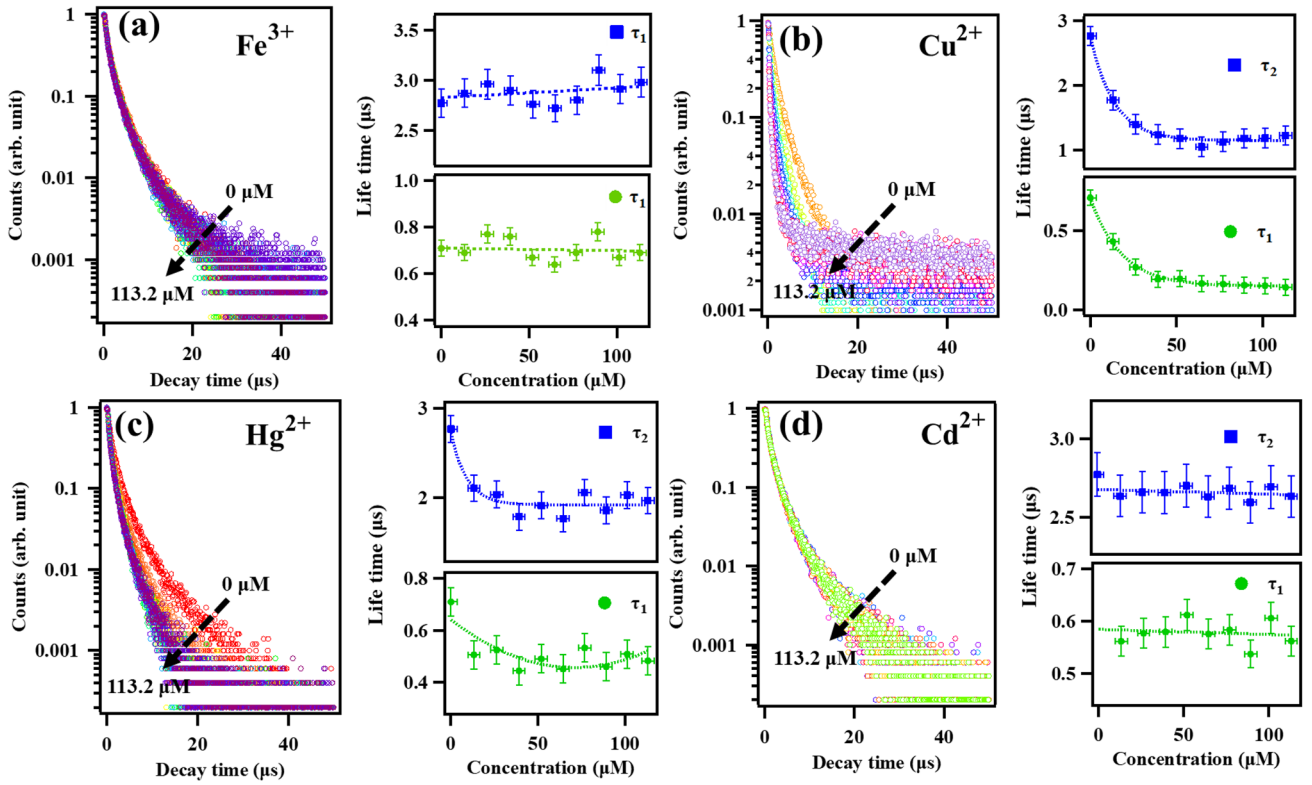

Fig. 3 TCSPC results to measure the phosphorescence decay profile and excited state lifetime values of AuAg-SG cluster during gradual addition (0 µM to 113.2 µM) of (**a**) Fe^{3+} ion, (**b**) Cu^{2+} ion, (**c**) Hg^{2+} ion and (**d**) Cd^{2+} ion

Table 1 The summary of excited state lifetime values of AuAg-SG cluster during gradual addition of Cu^{2+}, Fe^{3+}, Hg^{2+} and Cd^{2+} ions (0–113.2 μM) by using an excitation wavelength of 370 nm (spectra LED), and the emission was monitored at 604 nm

Conc	Cu^{2+}		Fe^{3+}		Hg^{2+}		Cd^{2+}	
μM	τ_1(μs)	τ_2(μs)	τ_1(μs)	τ_2(μs)	τ_1(μs)	τ_2(μs)	τ_1(μs)	τ_2(μs)
0	0.71 (62%)	2.77 (38%)	0.71 (62%)	2.77 (38%)	0.71 (62%)	2.77 (38%)	0.71 (62%)	2.77 (38%)
13.2	0.43 (58%)	1.78 (42%)	0.69 (64%)	2.87 (36%)	0.51 (65%)	2.10 (35%)	0.56 (59%)	2.63 (41%)
26.3	0.27 (64%)	1.40 (36%)	0.77 (69%)	2.96 (31%)	0.52 (70%)	2.03 (30%)	0.58 (62%)	2.65 (38%)
39.2	0.19 (71%)	1.24 (29%)	0.76 (69%)	2.90 (31%)	0.44 (67%)	1.78 (33%)	0.58 (60%)	2.66 (40%)
51.9	0.20 (72%)	1.18 (28%)	0.67 (56%)	2.76 (44%)	0.49 (73%)	1.91 (27%)	0.61 (63%)	2.70 (37%)
64.5	0.17 (77%)	1.10 (23%)	0.64 (60%)	2.72 (40%)	0.45 (71%)	1.76 (29%)	0.58 (61%)	2.63 (39%)
76.9	0.16 (84%)	1.13 (16%)	0.69 (58%)	2.80 (42%)	0.53 (78%)	2.05 (22%)	0.58 (61%)	2.68 (39%)
89.2	0.16 (89%)	1.18 (11%)	0.78 (66%)	3.10 (34%)	0.46 (74%)	1.86 (26%)	0.54 (60%)	2.60 (40%)
101.3	0.15 (89%)	1.19 (11%)	0.67 (62%)	2.91 (38%)	0.51 (78%)	2.03 (22%)	0.61 (61%)	2.70 (39%)
113.2	0.14 (92%)	1.22 (08%)	0.69 (62%)	2.98 (38%)	0.48 (77%)	1.96 (23%)	0.56 (59%)	2.63 (41%)

metal ions and understanding the photo physical events associated with it. To accomplish this target the solution phase titration of various metal salts were performed with these two clusters at room temperature (298 K) by simultaneously measuring their steady-state emission spectra as described in the experimental section. First the titration was performed with Au-SG cluster and the results are presented in Figs. S9 and S10. We could observe significant quenching (turn-off) of the emission peak for two metal ions (Fe^{3+} and Hg^{2+}) while other metal salts are innocent towards the emission quenching. Careful investigation revealed that Au-SG cluster is most effective for sensing Fe^{3+} followed Hg^{2+} with quenching efficiencies of 79% and 45% respectively. The normalized emission intensity (I_0/I) was also plotted against concentrations for these metal ions by following the Stern–Volmer equation (Eq. 1) (Fig. S9) and the calculated Stern – Volmer constants were found to be 4.6×10^5 M^{-1}(Fe^{3+}) and 1.95×10^4 M^{-1}(Hg^{2+}).

$$I_0(\lambda)/I(\lambda) = K_{SV}(\lambda)[Q] + 1 \quad (1)$$

[where $I_0(\lambda)$ is the PL intensity at a specified emission wavelength λ in the absence of a quencher, I(λ) denote the PL intensity at emission wavelength λ at a quencher concentration [Q], and $K_{SV}(\lambda)$ represents the Stern – Volmer quenching constant at emission wavelength λ.]

The lowest detection limit for Fe^{3+} and Hg^{2+} were found to be 100, 135 nM respectively. Similar emission spectroscopic titrations were also performed by taking AuAg-SG cluster as probe against all these metals salts under identical conditions (Fig. 4). Very interestingly we could observe emission quenching (turn-off) for Cu^{2+}, Fe^{3+} and Hg^{2+}, but emission enhancement (turn-on) for Cd^{2+} ion while all other metal salts cause negligible change of the emission intensity of AuAg-SG cluster (Figs. S11, S12, S13, S14 and S15). The calculated Stern – Volmer constants were found to be 4.88×10^5 M^{-1}(Fe^{3+}), 2.4×10^6 M^{-1}(Cu^{2+}) and 1.7×105 M^{-1}(Hg^{2+}) and –[4×10^3 M^{-1}] (Cd^{2+}). With respect to pristine AuAg-SG cluster, the emission quenching percentage in presence of Cu^{2+}, Fe^{3+} and Hg^{2+} metal ions are 99%, 72% and 69% respectively and emission enhancement for Cd^{2+} ion is 220%. The lowest detection limit for Cu^{2+}, Fe^{3+}, Hg^{2+} and Cd^{2+} were found to be 20, 90, 95 and 75 nM respectively. A comparative chart on detection limit for various metal ions reported previously by various metal clusters and the present work is shown in Table S1. The result is of high significance as these two luminescent clusters could be used as selective metal ion sensor with high sensitivity at neutral pH conditions. In addition, it would be interesting to understand the underlying mechanism of this differential sensing behaviour of Au and AuAg clusters. Especially the turn on sensing for Cd^{2+} ion by AuAg cluster may open up the strategy to synthesize a new class of trinuclear cluster with high emission quantum yield. The visual colour change of AuAg-SG cluster under UV (365 nm) light during gradual addition of Cd^{2+} ions (turn-on) and Fe^{3+} ions (turn-off) are also presented (Fig. S15).

Dynamic Light Scattering (DLS) and TCSPC Analysis

To understand the sensing mechanism we have measured the hydrodynamic diameter (D_h) and excited state life times (τ) of the both clusters during gradual addition of some selected metal salts. In general the luminescence quenching phenomenon occurs through photo-induced electron transfer (PET) process via static or dynamic interaction between probe and the analyte [42–50]. However, the turn-on sensing is uncommon and the underlying mechanism may be very distinct for different probes [51–53]. The TCSPC measurement was performed to record the excited state lifetime values of AuAg cluster upon gradual addition of Cu^{2+}, Fe^{3+}, Hg^{2+} and Cd^{2+}(Fig. 3 and Table 1). In parallel, DLS measurement was performed for Fe^{3+} (turn-off) and Cd^{2+} (turn-on) titrations with AuAg cluster to see any

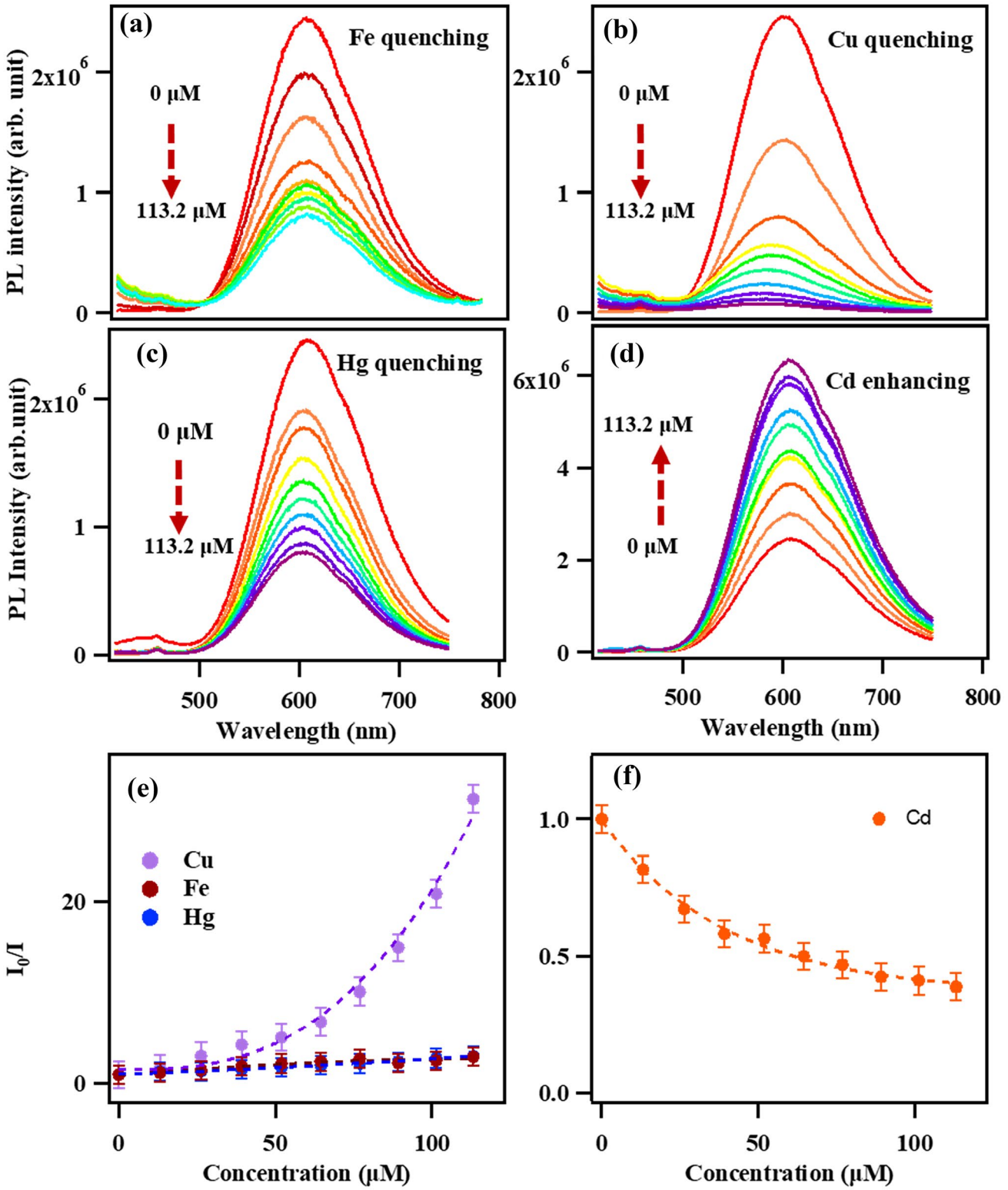

Fig. 4 Luminescence spectroscopic titration of AuAg-SG cluster with incremental addition (0 µM to 113.2 µM) of (**a**) Fe^{3+}, (**b**) Cu^{2+}, (**c**) Hg^{2+} and (**d**) Cd^{2+} respectively, in water at 298 K under neutral pH of 7.5; (**e**) and (**f**) are Stern–Volmer plots obtained for these metal ions from the above spectral intensities

change of the D_h values (Fig. 5). The τ values of pristine cluster (0.71 and 2.77 µs) decreases minutely after addition of 1.13 µM Cu^{2+} to 0.14 and 1.22 µs, and after addition of 1.13 µM Hg^{2+} to 0.48 and 1.96 µs. The τ value minutely increases to 0.69 and 2.98 µs after addition of same amount of Fe^{3+} and remains almost same (0.56 and 2.63 µs) after adding same amount of Cd^{2+} as shown in Table 1. The variation of τ_1 and τ_2 values of AuAg cluster upon varying addition of these four metal ions are also shown in Fig. 3. However, in all these studies the variation of τ values between pristine cluster and after addition of 1.13 µM metal salts is very minimal. The result clearly indicates static (ground state) interaction between the AuAg-SG cluster and metal ions. On the other hand the D_h value of pristine AuAg cluster is 2.5 nm, but after gradual addition of Fe^{3+} ion, it increases sharply and finally reaches to 1200 nm (Fig. 5). This clearly indicates that Fe^{3+} induces strong agglomeration by ligating with SG ligands (Scheme 1) and the emission quenching results through PET process from cluster to ligated Fe^{3+} ions. On the contrary, the D_h value of AuAg cluster remains same upon gradual addition of Cd^{2+} ions. We can postulate that here Cd^{2+} ions interacts with the cluster surface and forms an alloy rather than interaction with SG ligands. The enhanced luminescence originates from the cluster core due to formation of CdAuAg alloy with higher rigidity and hence lower vibrational relaxation. The TCSPC and DLS measurements of Au-SG cluster with gradual addition of Fe^{3+} ions were also recorded (Figs. S3 and S17) and the results are very identical with AuAg-SG cluster and Fe^{3+} ion. The τ values of pristine Au-SG cluster are 0.26 and 2.84 µs and after addition of 133.2 µM of Fe^{3+}, it remains almost same (0.25 and 2.85 µs) (Fig. S3) although the D_h value increases sharply from 2.5 nm to 415 nm (Fig. S17). We can postulate that Fe^{3+} binds with the SG ligands and through inter cluster linkages, high degree of agglomeration takes place in solution. From these analysis we came to conclusion that there are two distinct mechanisms operative here which is analyte (metal ion specific). For Cd^{2+} ion sensing by AuAg-SG cluster, the metal ion is binding with the cluster surface to form an alloy with turn-on luminescence response. This was further supported by isolating the cluster after titration with Cd^{2+}ion and finding the metal content through ICP-OES and ED-XRF experiments (Fig. S18 and Table S2).

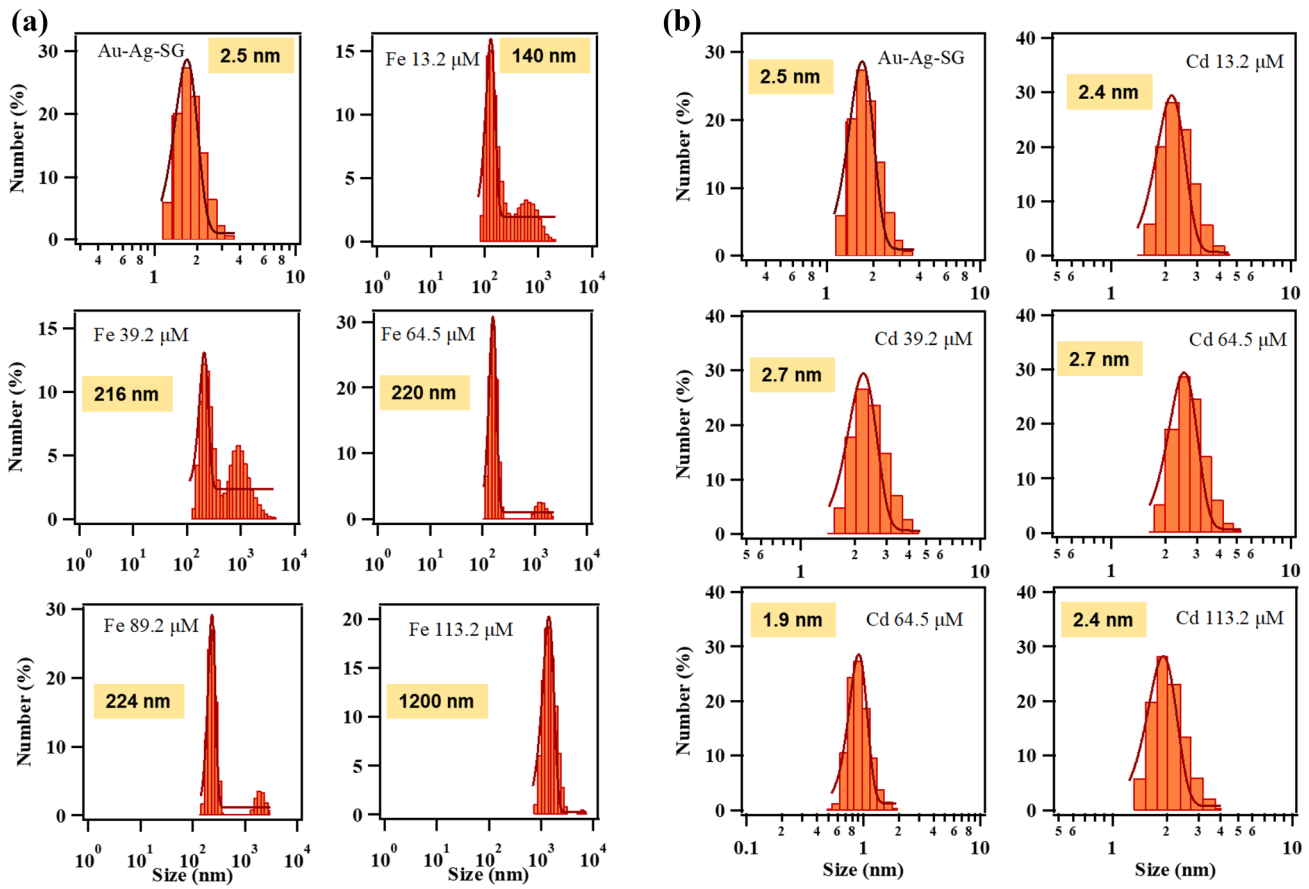

Fig. 5 Hydrodynamic diameter of aqueous solution of AuAg-SG cluster during gradual addition of Fe^{3+}ion (**a**) and Cd^{2+} ion (**b**)

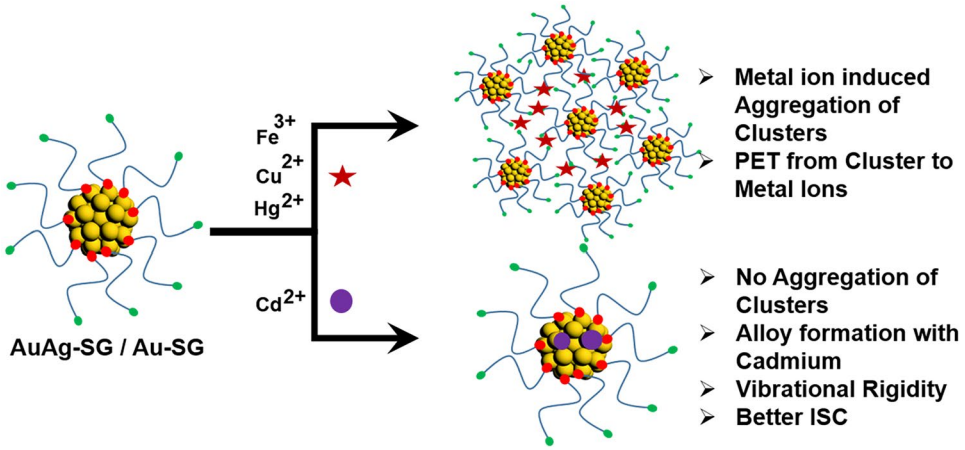

Scheme 1 Proposed mechanism of selective metal ion(s) induced emission quenching / enhancement of Au-SG/AuAg-SG clusters

The ICP-OES data and ED-XRF data shows the presence of Cd along with Au and Ag in the cluster implying its interaction the cluster surface. On the other hand other metal ions (Fe^{3+}, Cu^{2+}, Hg^{2+}) induced extensive cluster agglomeration through binding the SG ligands and results turn-off luminescence by PET process.

Conclusion

In conclusion, the present work successfully demonstrates the synthesis and sensing application of glutathione stabilized phosphorescent gold (Au-SG) and gold-silver (AuAg-SG) bimetallic nanoclusters for metal ions. Pronounced emission quenching is observed in case of metal ions of Fe^{3+}, Cu^{2+}, Hg^{2+}, whereas, the emission enhancement occurs while adding Cd^{2+} ions to AuAg cluster. High Stern – Volmer constant, low detection limit along with simple protocol, naked eye detection, low cost, fast processing time are very promising findings for their practical application. In addition to sensing application, the turn on sensing of Cd^{2+} ions by AuAg-SG cluster is a new finding and the mechanistic insight shows that a tri-metallic alloy cluster may be forming with much enhanced emission. The finding indicates the opportunity to synthesize highly luminescent Cd doped AuAg cluster with the possibility of their large scale synthesis and potential applications.

Supplementary Information The online version contains supplementary material available at https://doi.org/10.1007/s10895-022-03017-x.

Author Contributions SB, SP, IT did all the experimental works including synthesis, characterization and sensing studies of metal clusters, PM conceptualized the work, all the authors wrote the manuscript and PM did final corrections of the draft.

Funding This work was supported by Council of Scientific & Industrial Research (CSIR, New Delhi) (Project no. 01(2873)/17/EMR-II).

Data Availability The authors declare that the data supporting the findings of this study are available in the article and in the supplementary materials.

Declarations

Ethical Approval Not applicable.

Consent to Participate The work does not involve any form of study on human or animal species and hence no ethical clearance is needed.

Consent for publication The work does not contain any data from any individual person and hence no such permission is required.

Conflict of Interest The authors declare no conflict of interest.

References

1. Maity P, Xie S, Yamauchi M, Tsukuda T (2012) Stabilized gold clusters: from isolation toward controlled synthesis. Nanoscale 4:4027–4037. https://doi.org/10.1039/C2NR30900A
2. Luo Z, Zheng K, Xie J (2014) Engineering ultrasmall water-soluble gold and silver nanoclusters for biomedical applications. Chem Comm 50:5143–5155. https://doi.org/10.1039/C3CC47512C
3. Cui M, Zhao Y, Song Q (2014) Synthesis, optical properties and applications of ultra-small luminescent gold nanoclusters. Trends Analyt Chem 57:73–82. https://doi.org/10.1016/j.trac.2014.02.005
4. Jain PK, Huang X, El-Sayed IH, El-Sayed MA (2008) Noble metals on the nanoscale: optical and photothermal properties and some applications in imaging, sensing, biology, and medicine. Acc Chem Res 41:1578–1586. https://doi.org/10.1021/ar7002804
5. Bhattacharyya K, Mukherjee S (2018) Fluorescent metal nanoclusters as next generation fluorescent probes for cell imaging and drug delivery. Bull Chem Soc Jpn 91:447–454. https://doi.org/10.1246/bcsj.20170377
6. Resch-Genger U, Grabolle M, Cavaliere-Jaricot S, Nitschke R, Nann T (2008) Quantum dots versus organic dyes as fluorescent labels. Nat Methods 5:763–775

7. Huang Y, Fuksman L, Zheng J (2018) Luminescence mechanisms of ultrasmall gold nanoparticles. Dalton Trans 47:6267–6273. https://doi.org/10.1039/C8DT00420J
8. Zheng J, Zhou C, Yu M, Liu J (2012) Different sized luminescent gold nanoparticles. Nanoscale 4:4073–4083. https://doi.org/10.1039/C2NR31192E
9. Kang X, Zhu M (2019) Tailoring the photoluminescence of atomically precise nanoclusters. Chem Soc Rev 48:2422–2457. https://doi.org/10.1039/C8CS00800K
10. Wu Z, Jin R (2010) On the ligand's role in the fluorescence of gold nanoclusters. Nano Lett 10:2568–2573. https://doi.org/10.1021/nl101225f
11. Shellaiah M, Sun KW (2017) Luminescent metal nanoclusters for potential chemosensor applications. Chemosensors 5:36. https://doi.org/10.3390/chemosensors5040036
12. Brust M, Walker M, Bethell D, Schiffrin DJ, Whyman R (1994) Synthesis of thiol-derivatised gold nanoparticles in a two-phase liquid–liquid system. J Chem Soc, Chem Commun 7:801–802. https://doi.org/10.1039/C39940000801
13. Negishi Y, Kurashige W, Kamimura U (2011) Isolation and structural characterization of an octaneselenolate-protected Au_{25} cluster. Langmuir 27:12289–12292. https://doi.org/10.1021/la203301p
14. Müller CI, Lambert C (2011) Electrochemical and optical characterization of triarylamine functionalized gold nanoparticles. Langmuir 27:5029–5039. https://doi.org/10.1021/la1051244
15. Briant CE, Theobald BR, White JW, Bell LK, Mingos DM, Welch AJ (1981) Synthesis and X-ray structural characterization of the centred icosahedral gold cluster compound $[Au_{13}(PMe_2Ph)_{10}Cl_2](PF_6)_3$; the realization of a theoretical prediction. J Chem Soc, Chem Commun 201–202. https://doi.org/10.1039/C39810000201
16. Maity P, Tsunoyama H, Yamauchi M, Xie S, Tsukuda T (2011) Organogold clusters protected by phenylacetylene. J Am Chem Soc 133:20123–20125. https://doi.org/10.1021/ja209236n
17. Maity P, Takano S, Yamazoe S, Wakabayashi T, Tsukuda T (2013) Binding motif of terminal alkynes on gold clusters. J Am Chem Soc 135:9450–9457. https://doi.org/10.1021/ja401798z
18. Maity P, Sasai K, Dhital RN, Sakai H, Hasobe T, Sakurai H (2020) Excimer formation of aryl iodides chemisorbed on gold nanoparticles for the significant enhancement of photoluminescence. J Phys Chem Lett 11:1199–1203. https://doi.org/10.1021/acs.jpclett.9b03557
19. Negishi Y, Nobusada K, Tsukuda T (2005) Glutathione-protected gold clusters revisited: bridging the gap between gold (I) thiolate complexes and thiolate-protected gold nanocrystals. J Am Chem Soc 127:5261–5270. https://doi.org/10.1021/ja042218h
20. Yu Y, Luo Z, Chevrier DM, Leong DT, Zhang P, Jiang DE, Xie J (2014) Identification of a highly luminescent $Au_{22}(SG)_{18}$ nanocluster. J Am Chem Soc 136:1246–1249. https://doi.org/10.1021/ja411643u
21. Pyo K, Thanthirige VD, Yoon SY, Ramakrishna G, Lee D (2016) Enhanced luminescence of $Au_{22}(SG)_{18}$ nanoclusters via rational surface engineering. Nanoscale 8:20008–20016. https://doi.org/10.1039/C6NR07660B
22. Pyo K, Thanthirige VD, Kwak K, Pandurangan P, Ramakrishna G, Lee D (2015) Ultrabright luminescence from gold nanoclusters: rigidifying the Au (I)–thiolate shell. J Am Chem Soc 137:8244–8250. https://doi.org/10.1021/jacs.5b04210
23. Kumar S, Bolan MD, Bigioni TP (2010) Glutathione-stabilized magic-number silver cluster compounds. J Am Chem Soc 132:13141–13143. https://doi.org/10.1021/ja105836b
24. Zhang B, Chen C, Chuang W, Chen S, Yang P (2020) Size transformation of the $Au_{22}(SG)_{18}$ nanocluster and its surface-sensitive kinetics. J Am Chem Soc 142:11514–11520. https://doi.org/10.1021/jacs.0c03919
25. Yau SH, Ashenfelter BA, Desireddy A, Ashwell AP, Varnavski O, Schatz GC, Bigioni TP, Goodson T III (2017) Optical properties and structural relationships of the silver nanoclusters $Ag_{32}(SG)_{19}$ and $Ag_{15}(SG)_{11}$. J Phys Chem C 121:1349–1361. https://doi.org/10.1021/acs.jpcc.6b10434
26. Baksi A, Bootharaju MS, Chen X, Hakkinen H, Pradeep T (2014) $Ag_{11}(SG)_7$: A new cluster identified by mass spectrometry and optical spectroscopy. J Phys Chem C 118:21722–21729. https://doi.org/10.1021/jp508124b
27. Ungor D, Szilágyi I, Csapó E (2021) Yellow-emitting Au/Ag bimetallic nanoclusters with high photostability for detection of folic acid. J Mol Liq 338:116695. https://doi.org/10.1016/j.molliq.2021.116695
28. Zhang J, Yuan Y, Wang Y, Sun F, Liang G, Jiang Z, Yu SH (2015) Microwave-assisted synthesis of photoluminescent glutathione-capped Au/Ag nanoclusters: a unique sensor-on-a-nanoparticle for metal ions, anions, and small molecules. Nano Res 8:2329–2339
29. Fereja SL, Li P, Guo J, Fang Z, Zhang Z, Zhuang Z, Zhang X, Liu K, Chen W (2021) Silver-enhanced fluorescence of bimetallic Au/Ag nanoclusters as ultrasensitive sensing probe for the detection of folic acid. Talanta 233:122469. https://doi.org/10.1016/j.talanta.2021.122469
30. Mi W, Tang S, Jin Y, Shao N (2021) Au/Ag bimetallic nanoclusters stabilized by glutathione and lysozyme for ratiometric sensing of H_2O_2 and hydroxyl radicals. ACS Appl Nano Mater 4:1586–1595. https://doi.org/10.1021/acsanm.0c03053
31. Ganguly M, Jana J, Pal A, Pal T (2016) Synergism of gold and silver invites enhanced fluorescence for practical applications. RSC adv 6:17683–17703. https://doi.org/10.1039/C5RA26430H
32. Zhang XP, Huang KY, He SB, Peng HP, Xia XH, Chen W, Deng HH (2021) Single gold nanocluster probe-based fluorescent sensor array for heavy metal ion discrimination. J Hazard Matter 405:124259. https://doi.org/10.1016/j.jhazmat.2020.124259
33. Song Y, Li Y, Zhou M, Liu X, Li H, Wang H, Shen Y, Zhu M, Jin R (2021) Ultrabright Au@ Cu14 nanoclusters: 71.3% phosphorescence quantum yield in non-degassed solution at room temperature. Sci Adv 7:eabd2091. https://doi.org/10.1126/sciadv.abd20
34. Wang S, Meng X, Das A, Li T, Song Y, Cao T, Zhu X, Zhu M, Jin R (2014) A 200-fold quantum yield boost in the photoluminescence of silver-doped AgxAu25−x nanoclusters: the 13th silver atom matters. Angew Chem 126:2408–2412. https://doi.org/10.1002/ange.201307480
35. Wang Y, Su H, Ren L, Malola S, Lin S, Teo BK, Häkkinen H, Zheng N (2016) Site preference in multimetallic nanoclusters: incorporation of alkali metal ions or copper atoms into the alkynyl-protected body-centered cubic cluster $[Au_7Ag_8(C{\equiv}CtBu)_{12}]^+$. Angew Chem Int Ed 55:15152–151526. https://doi.org/10.1002/anie.201609144
36. Soldan G, Aljuhani MA, Bootharaju MS, AbdulHalim LG, Parida MR, Emwas AH, Mohammed OF, Bakr OM (2016) Gold doping of silver nanoclusters: a 26-Fold enhancement in the luminescence quantum yield. Angew Chem 128:5843–5847. https://doi.org/10.1002/ange.201600267
37. Lei Z, Guan ZJ, Pei XL, Yuan SF, Wan XK, Zhang JY, Wang QM (2016) An atomically precise $Au_{10}Ag_2$ nanocluster with Red–Near-IR dual emission. Chem Eur J 22:11156–11160. https://doi.org/10.1002/chem.201602403
38. Mitsui M, Arima D, Kobayashi Y, Lee E, Niihori Y (2022) On the origin of photoluminescence enhancement in biicosahedral Ag_xAu_{25-x} nanoclusters (x = 0–13) and their application to triplet-triplet annihilation photon upconversion. Adv Opt Mater. https://doi.org/10.1002/adom.202200864
39. Wang Z, Zhu Z, Zhao C, Yao Q, Li X, Liu H, Du F, Yuan X, Xie J (2019) Silver doping-induced luminescence enhancement and red-shift of gold nanoclusters with aggregation-induced

emission. Chem Asian J 14:765–769. https://doi.org/10.1002/asia.201801624
40. Qian S, Wang Z, Zuo Z, Wang X, Wang Q, Yuan X (2022) Engineering luminescent metal nanoclusters for sensing applications. Coord Chem Rev 451:214268. https://doi.org/10.1016/j.ccr.2021.214268
41. Kubavat J, Thakarda J, Tyagi T, Bhowmik S, Maity P (2021) Selective sensing of thiols by aryl iodide stabilized fluorescent gold cluster through turn-off excimer emission caused by ligand displacement. J Chem Sci 133:1–1
42. Thakarda J, Dave P, Bhowmik S, Kubavat J, Maity P (2021) 4-Iodophenylboronic acid stabilized gold cluster as a new fluorescent chemosensor for saccharides based on excimer emission quenching. J Fluoresc 31:447–454
43. Thakarda J, Agrawal B, Anil D, Jana A, Maity P (2020) Detection of trace-level nitroaromatic explosives by 1-pyreneiodide-ligated luminescent gold nanostructures and their forensic applications. Langmuir 36:15442–15449. https://doi.org/10.1021/acs.langmuir.0c03117
44. Dave P, Agrawal B, Thakarda J, Bhowmik S, Maity P (2019) An organometallic ruthenium nanocluster with conjugated aromatic ligand skeleton for explosive sensing. J Chem Sci 131:1–8
45. Srivastav AK, Agrawal B, Swami B, Agrawal YK, Maity P (2017) Ligand exchange synthesis of organometallic Rh nanoparticles and application in explosive sensing. J Nanoparticle Res 19:1–8
46. Zhuang H, Jiang X, Wu S, Wang S, Pang Y, Huang Y, Yan H (2022) A novel polypeptide-modified fluorescent gold nanoclusters for copper ion detection. Sci Rep 12:6624
47. Das NK, Ghosh S, Priya A, Datta S, Mukherjee S (2015) Luminescent copper nanoclusters as a specific cell-imaging probe and a selective metal ion sensor. J Phys Chem C 119:24657–24664. https://doi.org/10.1021/acs.jpcc.5b08123
48. Yang Y, Han A, Li R, Fang G, Liu J, Wang S (2017) Synthesis of highly fluorescent gold nanoclusters and their use in sensitive analysis of metal ions. Analyst 142:4486–4493. https://doi.org/10.1039/C7AN01348E
49. Guo C, Irudayaraj J (2011) Fluorescent Ag clusters via a protein-directed approach as a Hg (II) ion sensor. Anal Chem 83:2883–2889. https://doi.org/10.1021/ac1032403
50. Zhang G, Li Y, Xu J, Zhang C, Shuang S, Dong C, Choi MM (2013) Glutathione-protected fluorescent gold nanoclusters for sensitive and selective detection of Cu^{2+}. Sens Actuators B Chem 183:583–588. https://doi.org/10.1016/j.snb.2013.04.023
51. Mohanty JS, Chaudhari K, Sudhakar C, Pradeep T (2019) Metal-ion-induced luminescence enhancement in protein protected gold clusters. J Phys Chem C 123:28969–28976. https://doi.org/10.1021/acs.jpcc.9b07370
52. Peng Y, Wang M, Wu X, Wang F, Liu L (2018) Methionine-capped gold nanoclusters as a fluorescence-enhanced probe for cadmium (II) sensing. Sensors 18:658. https://doi.org/10.3390/s18020658
53. Akshath US, Bhatt P, Singh SA (2020) Differential interaction of metal ions with gold nanoclusters and application in detection of cobalt and cadmium. J Fluoresc 30:537–545. https://doi.org/10.1007/s10895-020-02509-y
54. Yin Z, Wang Z, Dai X, Liu N, Wang S, Li G, Du F, Yuan X (2020) Highly luminescent AuAg nanoclusters with aggregation-induced emission for high-performance white LED application. ACS Sustain Chem Eng 8:15336–15343. https://doi.org/10.1021/acssuschemeng.0c05722